

# INTERACTIONS OF POINT DEFECTS WITH DISLOCATIONS IN SODIUM CHLORIDE CRYSTALS

著者	TATENO Hiroto
journal or publication title	鹿児島大学理学部紀要. 数学・物理学・化学
volume	14
page range	57-71
別言語のタイトル	NaCl単結晶中の点欠陥と転位の相互作用
URL	<a href="http://hdl.handle.net/10232/00003979">http://hdl.handle.net/10232/00003979</a>

# INTERACTIONS OF POINT DEFECTS WITH DISLOCATIONS IN SODIUM CHLORIDE CRYSTALS

By

Hiroto TATENO

(Received Sep. 30, 1981)

## Abstract

An attempt has been made to study the behaviour of dislocation atmosphere in NaCl crystals by internal friction and conductivity measurements. The measurements have been carried out on both pinning and unpinning processes by Marx's oscillator method using an automatic control circuit. The results indicate that the number of pinners on dislocation increases or decreases proportionally to  $1/3$  power of time with the activation energy,  $0.25 \pm 0.05$  eV, in both processes. From a migration energy of divalent impurity-vacancy complex,  $E_m$ , in pure NaCl crystals, and a binding energy of the complex,  $E_b$ , an activation energy for exchange between the divalent impurity and neighbouring vacancy is deduced as  $E_a = E_m + E_b = 0.82 \pm 0.05$  eV. The  $t^{1/3}$  dependence of unpinning and pinning process of point defects is quantitatively explained, assuming that the distribution of divalent impurity-atmosphere is controlled by elastic interaction potential, and not by the electrical potential due to a dislocation.

## § 1. Introduction

The behaviours of point defects with dislocations in single crystals have been widely studied with internal friction measurements, especially anelastic properties versus time or strain amplitude after either plastic deformation or high strain amplitude oscillations were presented<sup>1,2,3</sup>). First, Cottrell and Bilby<sup>4</sup>) showed that the pinning process of fresh dislocations by homogeneously distributed point defects is proportional to  $2/3$  power of aging time at least in an initial stage of the aging process and they explained in terms of the formation of the atmosphere. The  $2/3$  power law was also observed in deformed NaCl crystals by Phillips and Pratt,<sup>3</sup>) and in deformed LiF by Carpenter<sup>5</sup>) and by Guenin et al.<sup>6</sup>) On the other hand, the pinning process of dislocations in deformed and aged specimens after the oscillation in a breakaway region was reported to obey the  $1/3$  power law in LiF by Carpenter<sup>7</sup>), and in AgCl by Kim et al.<sup>8</sup>) The possibility of  $t^{1/3}$  law for a planar distribution of the atmosphere was proposed by Carpenter and was explained by Kim et al., using the one dimensional small perturbation model. But in this model, the conservation of the number of point defects around dislocations is not satisfied before and after excitation.

\* Department of Physics, Kagoshima University, Kagoshima Japan

So the relation between the  $2/3$  and the  $1/3$  power laws has not been clear yet. In this experiment, in order to clear above relations, the internal friction of NaCl single crystals is continuously measured by constant amplitude during unpinning and pinning process. And the origins of  $2/3$  and  $1/3$  power laws will be discussed on the basis of present experimental results. In addition to internal friction measurements, the ionic conductivity of NaCl single crystals is also measured and we shall discuss on the diffusion of point defects around dislocations.

## § 2. Experimental procedure

In order to observe the unpinning and pinning processes of dislocation in NaCl crystals, internal friction was measured with a Marx's standard four-component oscillator<sup>9)</sup> operating at the fundamental longitudinal frequency 50 KHz. The frequency matched specimen was cemented with Araldite to a fused quartz rod, below which a quartz drive crystal and a quartz gauge crystal were cemented.

Internal friction was measured in the following way. After the damping was continuously measured at a constant strain amplitude in the breakaway region for 3 hours, the strain amplitude was changed into a lower value, which is about  $10^{-4}$  times the breakaway amplitude, and again the damping was continuously measured for 1~3 hours. These measurement were carried out at constant temperatures within  $\pm 0.5^\circ\text{C}$  in the range of  $-92^\circ\text{C} \sim 114^\circ\text{C}$ .

Both resonant frequency and strain amplitude were automatically controlled by the analogue computer method.<sup>10)</sup> The entire resonator system was set in a vacuum chamber. The changes in both resonant frequencies and dampings with time were traced with a  $X-t$  recorder. An ingot crystal,  $130^t \times 100$  mm, was made from special grade reagent NaCl in a Bridgeman-Stockbarger furnace with nitrogen atmosphere. The concentration of free divalent impurities has been estimated to be about 6 ppm from the ionic conductivity, and the concentration of Ca-ions was about 15 ppm by the estimation of the atomic absorption analysis. The specimens surrounded by {001} planes,  $5 \times 5 \times 45$  mm<sup>3</sup> in size, were made by cleaving the ingot and by polishing on wet paper. They were annealed at about  $700^\circ\text{C}$  for 10 hours in nitrogen atmosphere, and then cooled down to room temperature with the rate of  $10^\circ\text{C}/\text{hour}$ . The specimens thus treated were compressed about 1.5% in length, and were aged at  $250^\circ\text{C}$  for 10 hours. The dislocation densities of the specimens before and after the compression were about  $10^5$  cm/cm<sup>3</sup> and  $10^6$  cm/cm<sup>3</sup>, respectively. Figure 1 shows the typical etch-pit pattern of these specimens.

In order to measure the binding energy between a cation vacancy and a divalent impurity, the ionic conductivity was measured on a specimen of about  $10 \times 10 \times 1$  mm<sup>3</sup>, which was cleaved from a side of the sample of internal friction measurement and was polished by wet paper. Electrodes employed were carbon paint. The whole system was assembled into a vacuum furnace and then nitrogen gas was charged into the furnace to prevent evaporation of NaCl. Measurements were made with increasing

and decreasing temperature after a thermal annealing at 400°C for 3 hours, with the normal and the reversed polarity of applied dc voltage.

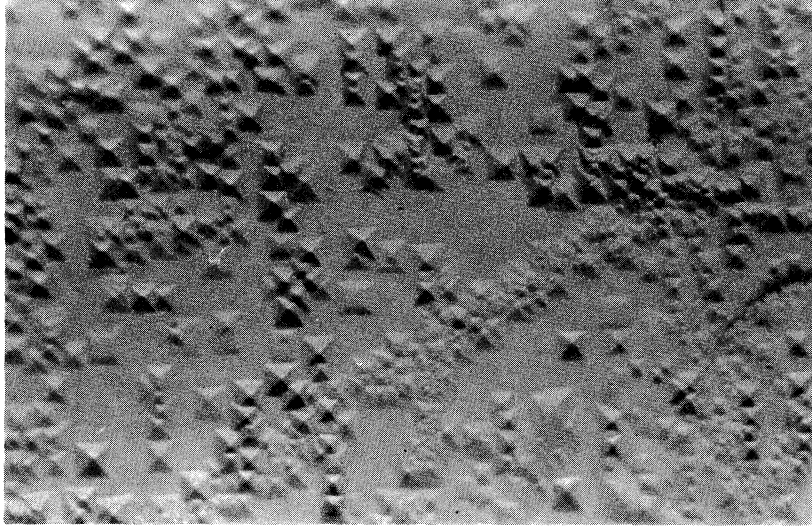


Fig. 1. Dislocation etch pits just after the compression; this photo was taken at the magnification of 600. The dislocation density is estimated to be of the order of  $10^6/\text{cm}^2$ .

### § 3. Experimental Results

The strain-dependent dampings,  $A_H$ , of NaCl crystals were measured at various temperatures by a strain amplitude  $\sim 10^{-4}$ . It was found that damping at constant temperature increases with time. This increase of damping may be ascribed to the increase of mean length of dislocation segments with time. After the above measurements, the strain-independent dampings,  $A_I$ , in pinning process at various temperatures were measured at the strain amplitude  $\sim 10^{-8}$ . In this case, the value of  $A_I$  decreases with time. This may show that the mean length of dislocation segments decreases with time.

The relations between time  $t$  and  $A_I$  are shown in Fig. 2 for various temperatures, where the vertical axis is taken in  $\ln A_H$  and the horizontal axis  $t^{1/3}$ . The relationship between time and  $A_I$  is illustrated in Fig. 3 for various temperatures, where the vertical axis is taken  $(A_I/A_0)$  (see equation (4, 24)) and the horizontal axis  $t^{1/3}$ , where  $\beta$  is the strain amplitude independent decrement at  $t=0$ . In these figures,  $t^{1/3}$  plot is more suitable than  $t^{2/3}$  plot to obtain the linear relation between time and either  $\ln A_H$  or  $(A_I/A_0)^{-1/4}$ .

As shown in the next section (the reader should refer to page 68 for further details), the rate of unpinning and pinning parameter  $\beta$  in the present experiments could be given by

$$\beta = (2\rho)^3 \frac{4AD}{\pi kT}, \quad (3.1)$$

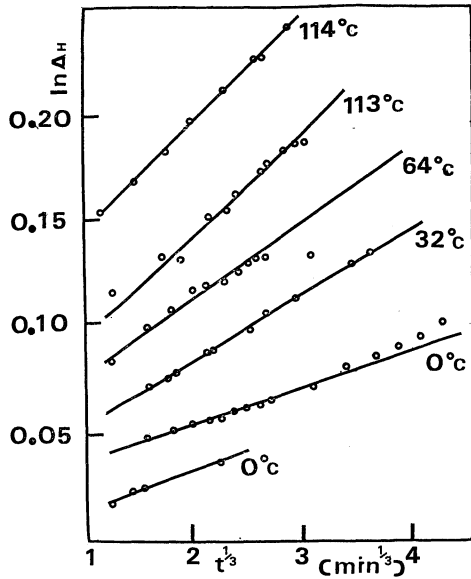


Fig. 2. The relation between  $\ln \Delta_H$  and  $t^{1/3}$  for various temperatures. The specimen was deformed by 1.5% in length and aged.

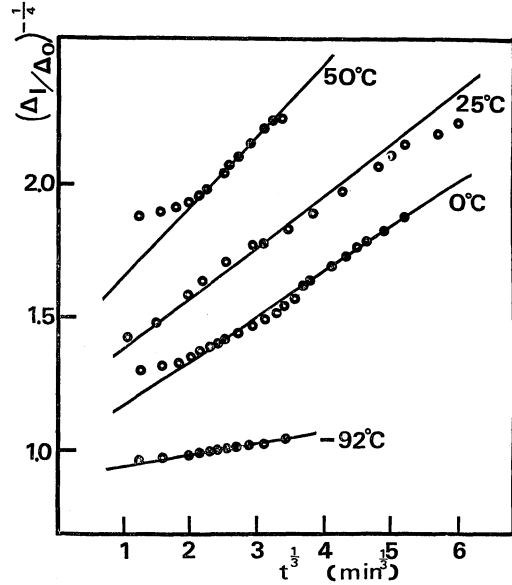


Fig. 3. The relation between  $(\Delta_I/\Delta_0)^{-1/4}$  and  $t^{1/3}$  for 1.5% deformed crystal are shown for various temperatures. The values of  $\Delta_I$  were measured after the high amplitude excitation.

here,  $\rho$  is the density of point defects,  $A$  is the constant, and  $D$  is the diffusion constant as written

$$D = D_0 \exp(-E_m/kT). \quad (3.2)$$

Both parameters,  $\beta$  can be obtained from the slope of Fig. 2 and Fig. 3 respectively. The relation between  $\ln \beta T$  and  $1/T$ , shown in Fig. 4 and Fig. 5, shows straight lines whose slopes give the migration energy,  $E_m = 0.25 \pm 0.05$  eV.

The ionic conductivity was measured from room temperature to melting point. Figure 6 shows  $\ln \sigma T$  vs  $1/T$  for NaCl, where  $\sigma$  is the conductivity, the four temperature regions I, II, III, and IV are indicated. In region I, which is known as the intrinsic region, the electrical conductivity,  $\sigma$ , is given by

$$\sigma = ne\mu = n \left( \frac{4e^2 g^2 f_0}{kT} \right) \exp(-E_{mc}/kT), \quad (3.3)$$

where  $n$  is the concentration of cation vacancies,  $\mu$  is the mobility of vacancy,  $g$  is the distance between nearest-neighbor cation and anion,  $E_{mc}$  is the migration energy of a cation vacancy,  $f_0$  is a frequency factor, and  $e$  and  $kT$  have their usual meaning.<sup>11)</sup> The expression for  $n$  is given by

$$n \propto \frac{1}{N} \exp(-E_s/2kT), \quad (3.4)$$

where  $E_s$  is the energy of formation of a Schottky pair, and  $N$  is the concentration of

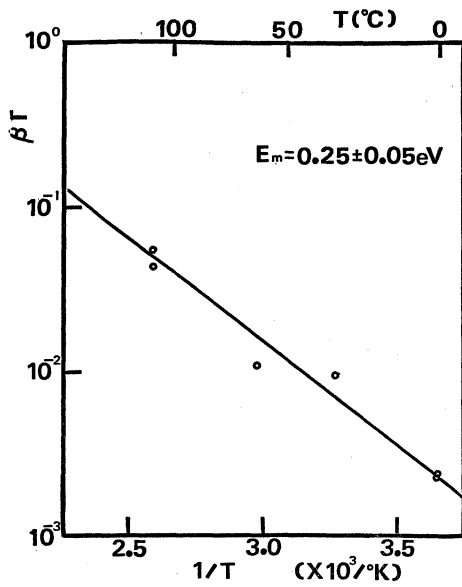


Fig. 4. The relation between the unpinning rate in the amplitude dependent decrement and the reciprocal temperature. The migration energy is estimated to be  $0.25 \pm 0.05$  eV.

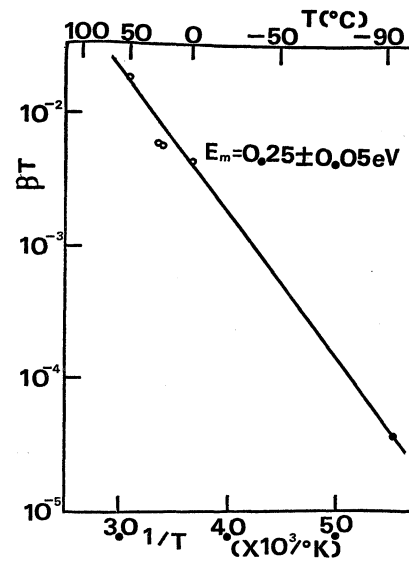


Fig. 5. The relation between the decay rate in the amplitude independent decrement and the reciprocal temperature. The migration energy estimated from this relation is  $0.25 \pm 0.05$  eV.

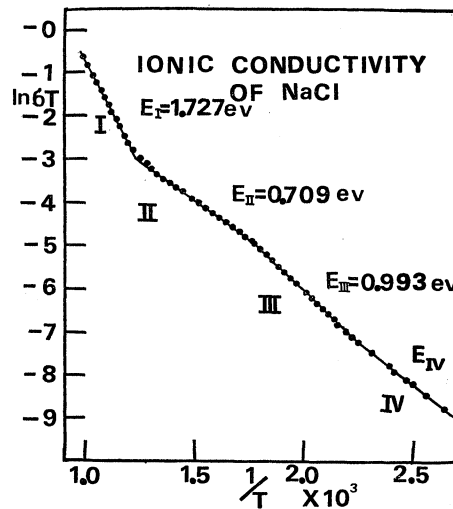


Fig. 6. The conductivity plots of an NaCl crystal: The concentration of CaCl is 15 ppm mole fraction. Four temperature regions and their activation energies are shown.

cation lattice sites. Combining equations (3.3) and (3.4) show that the effective activation energy,  $E_I$  for region I is written by

$$E_I = E_{mc} + \frac{1}{2} E_s. \tag{3.5}$$

In region II, the concentration of cation vacancies is a constant, and equals to the

total concentration of divalent metallic impurities. Therefore, the effective activation energy,  $E_{II}$  is equal to  $E_{mc}$ .

In region III, the association of divalent impurity ion and cation vacancy form a neutral complex. The effect of the association reaction on the conductivity is calculated for dilute solution, and the concentration of cation vacancies,  $n$  is expressed as

$$n \sim \exp(-E_b/2kT), \quad (3.6)$$

where  $E_b$  is the binding energy between vacancy and divalent impurity. From equations (3.3) and (3.6) the effective activation energy is given by

$$E_{III} = E_{mc} + \frac{1}{2} E_b. \quad (3.7)$$

In region IV, the majority of the impurities will be present in a well ordered aggregate phase composed of impurity ions, cation vacancies, and sodium and chlorine ions.

From the gradient of straight lines in four regions I, II, III, and IV in Fig. 6 effective activation energies are calculated and estimated as

$$E_I = 1.727 \text{ eV},$$

$$E_{II} = 0.709 \text{ eV},$$

$$E_{III} = 0.993 \text{ eV}.$$

The binding energy  $E_b=0.568$  eV is obtained by referring to equation (3.7).

## § 4. Discussion

### 4.1 Unpinning process

The distribution of point defects around a static dislocation is given by

$$C_s(r, \theta) = C_\infty \exp - U(r, \theta)/kT, \quad (4.1)$$

where  $C_\infty$  is the concentration of point defects at a large distance from the dislocation, and  $U(r, \theta)$  is the interaction energy between a point defect at  $(r, \theta)$  and the dislocation at  $(r=0)$ . Let us consider the motion of an edge dislocation along Z-axis under an oscillatory stress perpendicular to Z-axis on its slip plane X-Z. This model is illustrated in Fig. 7. Then the time interval  $\Delta t$  in which the dislocation is found in the region  $x$  and  $x+\Delta x$  is expressed as

$$\Delta t = 2 \left| \frac{\Delta x}{v} \right| = \left| \frac{2\Delta x}{\omega \xi \sin \omega t} \right| = \frac{2\Delta x}{\omega \sqrt{\xi^2 - x^2}}, \quad (4.2)$$

where  $x$  is the displacement of dislocation with respect to Z-axis,  $\xi$  is the amplitude of the vibrating dislocation,  $v$  and  $\omega$  are velocity and angular frequency of the dislocation, respectively. Therefore the probability density of periodic oscillation which is restricted in X-axis becomes

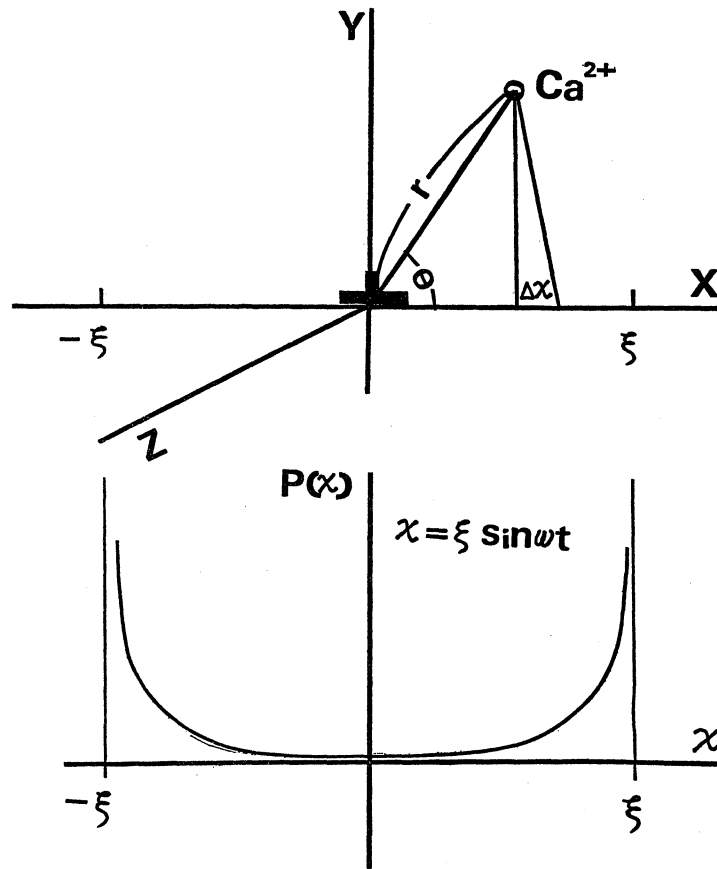


Fig. 7. The displacement of a dislocation from its equilibrium position is given by  $\pm\xi$ . The dislocation is along Z-axis. The effective interaction between the vibrating dislocation and  $\text{Ca}^{2+}$  at  $(x, y)$  is proportional to the time average of periodic oscillations  $P(x)$

$$P(x) = \frac{2A\chi}{\tau\omega\sqrt{\xi^2 - \chi^2}}, \quad (4.3)$$

where  $\tau$  is the period of oscillation. This is schematically shown in Fig. 7. We suppose, here, that the main term of the interaction between the edge dislocation and the point defect is elastic, because we imagine the divalent-impurity vacancy complex as the pinner. If  $r$  is the radial distance between a point defect and the core of an edge dislocation, the interaction between them can be approximated by the equation

$$U(r, \theta) = -\frac{A}{r} \sin \theta, \quad (4.4)$$

where  $A$  is appropriately chosen constant. Then the effective interaction potential  $U_m(x, y)$  between the vibrating dislocation and the point defect at  $(x, y)$  is the time average of periodic oscillation, which is the convolution of equations (4.3) and (4.4). Thus we obtained

$$U_m(x, y) = \frac{A}{\pi} \int_{-\xi}^{\xi} \frac{-y}{(x-\chi)^2 + y^2} \frac{1}{\sqrt{\xi^2 - \chi^2}} d\chi, \quad (4.5)$$



and  $\xi$  is written as

$$\xi = \frac{\varepsilon \Delta_H}{bA}, \quad (4.6)$$

where  $\varepsilon$  is the strain amplitude,  $\Delta_H$  the internal friction in the breakaway region of strain amplitude,  $A$  and  $b$  the dislocation density and the magnitude of Burgers vector, respectively.

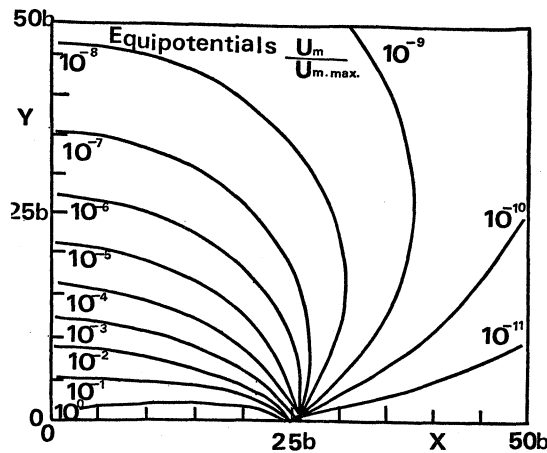


Fig. 8. Normalized equipotential lines of the first quadrant due to the motion of an edge dislocation along Z-axis, which is vibrated under an oscillatory stress on its slip plane, X-Z. The amplitude, is  $\pm 25$  burgers vectors.

The equipotential lines calculated from equation (4.5) are shown in Fig. 8. If the relaxation time of point defects is longer than the vibrating period of dislocations, the concentrations of divalent-impurities around a vibrating dislocation is given by

$$C_m(s, \theta) = C_\infty \exp - U_m(r, \theta)/kT. \quad (4.7)$$

This assumption will be explained as follows. In the low concentration, and the crystal not hot enough to be intrinsic, the divalent impurity ion can only diffuse, when it is associated with a vacancy. According to Nowick,<sup>12)</sup> the divalent impurity diffusion coefficient  $D$  is given by

$$D = a^2 \nu_0 f \exp(-E_a/kT) C_\infty \exp(E_b/kT), \quad (4.8)$$

here,  $a$ ,  $f$ , and  $D_0$  are the lattice parameter, correlation factor and the Debye frequency, respectively.  $E_a$  is the activation energy for the exchange of the impurity atom with neighbouring vacancy.  $E_b$  is the impurity vacancy association energy.

The temperature region of internal friction measurements corresponds to the region IV of conductivity measurement in Fig. 6. In this region, the impurities in the solution are segregated or precipitated out from the solid solution.<sup>13)</sup>

Thus the effective concentration of the diffusible impurity in solution,  $C_E$ , is considered to be much smaller than  $C_\infty$ . The relaxation time  $\tau'$  of point defects is given by

$$\begin{aligned}\tau' &= [\nu_0 \exp(-E_a/kT) C_\infty \exp(E_b/kT)]^{-1} \\ &= 1.1 \times 10^{-3} \text{ sec},\end{aligned}\quad (4.9)$$

here,  $\nu_0$ ,  $T$  and  $C_\infty$  are, respectively,  $10^{12}$  Hz,  $300^\circ\text{K}$  and 15 ppm. Now  $(E_a - E_b)$  is obtained by this work as  $0.25 \pm 0.05$  eV. Hence, the relaxation time of point defect is longer than the vibrating period of dislocation,  $2 \times 10^{-5}$  sec at 50 kHz.

On the other hand, the concentration of divalent-impurities around a static dislocation,  $C_r$ , is given by

$$C_s = C_E \exp - \frac{U(r, \theta)}{kT}. \quad (4.10)$$

When a stationary dislocation is suddenly vibrated by breakaway amplitude, then the imaginary concentration  $C_{s-m}$  is produced and is written as

$$C_{s-m} = C_s - C_m. \quad (4.11)$$

Figure 9 shows  $C_{s-m}$ .

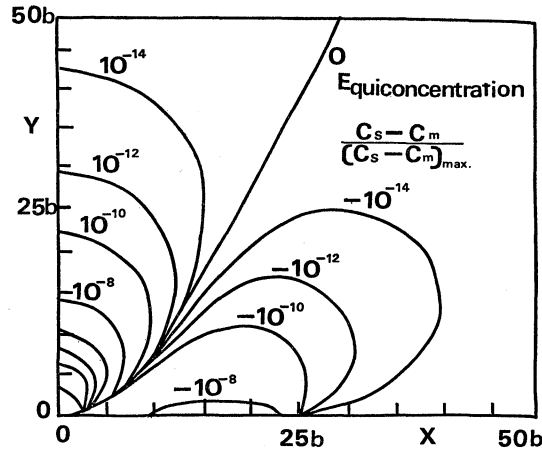


Fig. 9. Normalized equiconcentration lines of the difference between  $C_s$  and  $C_m$ , produced due to the motion of an edge dislocation along Z-axis, which is vibrating under an oscillatory stress on its slip plane X-Z. The amplitude is  $\pm 25$  burgers vectors.

Since a flow of divalent-impurities is caused by  $C_{r-m}$ . One obtains the following relation

$$\frac{1}{D} \frac{\partial C_{s-m}}{\partial t} = \nabla^2_{r,\theta} C_{s-m}, \quad (4.12)$$

where  $D$  is the diffusion coefficient of the divalent-impurities. The analytical solution of equation (4.12) is given by

$$C_{s-m}(x, y, t) = \int_{-\infty}^{\infty} \int_{-\infty}^{\infty} C_{s-m}(X, Y, 0) \frac{1}{2\pi Dt} \exp - \frac{(x-X) + (y-Y)^2}{4Dt} dX dY. \quad (4.13)$$

We solved equation (4.13), and obtained the number of divalent-impurities,  $N(t)$ , in the effective area of pinning around the dislocation line, which decreases with  $t^{1/3}$  dependence,

$$N(t) = \int_{-x_0}^{x_0} \int_{-y_0}^{y_0} C_{s-m}(x, y, t) dx dy, \quad (4.14)$$

where  $\pm x_0$  and  $\pm y_0$  are effective distances of pinning around the dislocation line. We showed a typical example of  $N(t)$  vs.  $t$  in Fig. 10. They have a simple proportional relation in initial stage. Thus, we get from Fig. 10

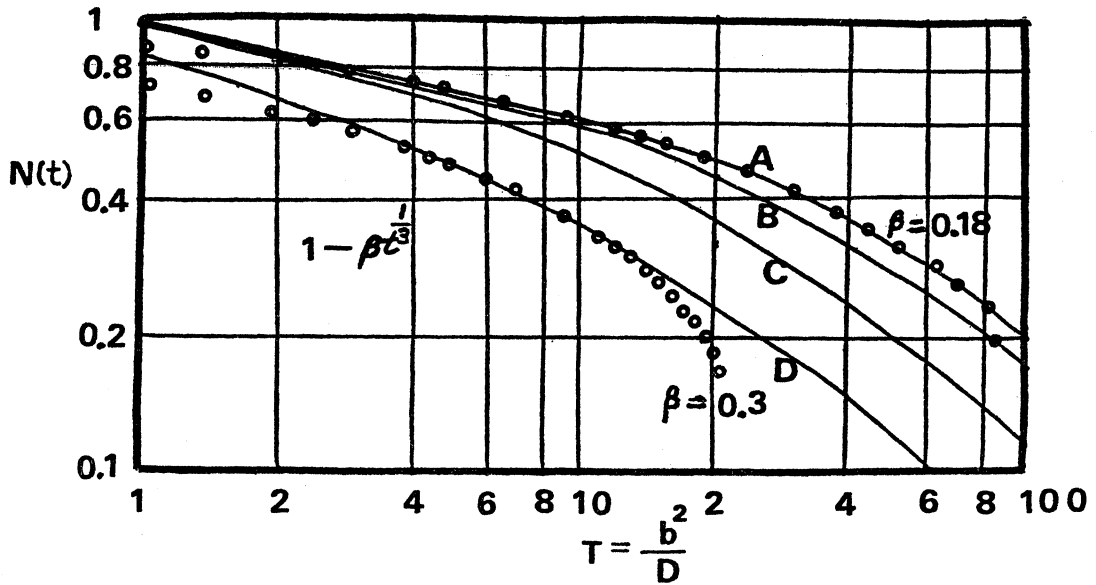


Fig. 10. The kinetics of the divalent impurity removed from the dislocation cores as a function of the reduced time:  $T = b^2/D$ . The full curves shown here are for various values of pinning region parameter  $(x, y)$ : Curves A,  $(\pm 6b, 1b)$ , B,  $(\pm 4b, 1b)$ , C,  $(\pm 2b, 1b)$ , and D,  $(\pm 1b, 1b)$ .

$$N(t) = N(0) [1 - (\beta t)^{1/3}], \quad (4.15)$$

where  $\beta$  is a constant.

According to Granato, Hikata and Lücke theory,<sup>14)</sup> the strain-dependent dampings  $\Delta_H$  is given by

$$\Delta_H = \frac{C_1}{L_c^2 \varepsilon} \exp - \frac{C_2}{L_c \varepsilon}, \quad (4.16)$$

where  $L_c$  is the mean free length of dislocation between weak pinning defects,  $\varepsilon$  is the vibration amplitude, and  $C_1$  and  $C_2$  are constants. The relation between  $L_c$  and  $N(t)$  is shown by

$$1/L_c = N(t). \quad (4.17)$$

If equation (4.16) is rearranged, using equations (4.15) and (4.17),

$$A_H = \frac{\beta^2 C_1 t^{2/3}}{\varepsilon} \exp - \frac{C_2 N(0)}{\varepsilon} [1 - (\beta t)^{1/2}]. \quad (4.18)$$

## 4.2 Pinning process

The equiconcentration line calculated from equation. (4.7) are shown in Fig. 11. In this figure, it is seen that the divalent-impurities are almost localized along the slip direction within the region of  $\pm \xi$  at constant concentration. For this reason, the divalent-impurities can be assumed to drift back to core region from the X-axis along the orbit of  $r=r_0 \cos \theta$ , where  $r_0$  is shown in Fig. 12. The drift velocity of divalent-impurities toward the dislocation is written as

$$v = (D/kT) [-V_{r,\theta} U(r, \theta)] = (D/kT) (F_r + F_\theta), \quad (4.19)$$

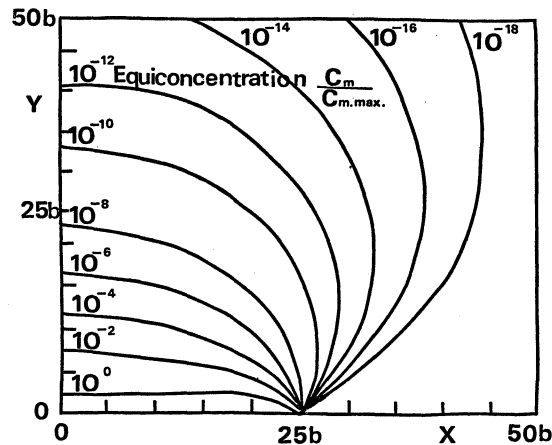


Fig. 11. Normalized equiconcentration lines of the first quadrant due to the motion of an edge dislocation along Z-axis, which vibrated under an oscillatory stress on its slip plane, X-Z. The amplitude is  $\pm 25$  burgers vectors.

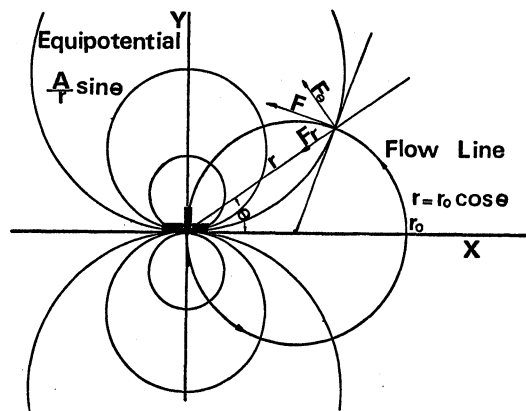


Fig. 12. Flow lines orthogonal to equipotentials indicate the direction of defect flow in the stress field of an edge dislocation due to the drift interaction. Illustration of notations in equations (4.19) and (4.20).

where  $F_r$  and  $F_\theta$  are the drift motive forces in polar coordinates as shown in Fig. 12. The time  $\Delta t$  which is required for a point defect to drift back at an orbit length  $\Delta l$  is shown as

$$\Delta t = \frac{\Delta l}{V} = \frac{kT}{D} \frac{\sqrt{(rd\theta)^2 + (dr)^2}}{\sqrt{F_r^2 + F_\theta^2}} = \frac{kT}{AD} r_0^3 \cos^2 \theta d\theta. \quad (4.20)$$

This is integrated over the limits, 0 to  $\pi/2$ ,

$$t = \frac{kT}{AD} r_0^3 \int_0^{\pi/2} \cos^2 \theta d\theta = \frac{kT}{AD} r_0^3 \frac{\pi}{4}, \quad (4.21)$$

or

$$r_0 = \left( \frac{4AD}{\pi kT} \right)^{1/3} t^{1/3}. \quad (4.22)$$

We obtain the amount of pinners,  $N(t)$ , which have arrived at the unit length of dislocation by time  $t$ .

$$N(t) = \rho 2r_0 = 2\rho \left( \frac{4AD}{\pi kT} \right)^{1/3} t^{1/3}, \quad (4.23)$$

where  $\rho$  is the density of point defects in the range of  $\pm\xi$  along the slip direction.

According to the Granato, Hikata and Lücke theory,<sup>14)</sup> the amplitude-independent decrement is given by

$$\begin{aligned} A_I &= A_0 [1 + N(t)]^{-4} = A_0 \left[ 1 + (2\rho) \left( \frac{4AD}{\pi kT} \right)^{1/3} t^{1/3} \right]^{-4} \\ &= A_0 [1 + (\beta t)^{1/3}]^{-4}, \end{aligned} \quad (4.24)$$

where  $\beta$  is the recovery parameter which is given by

$$\begin{aligned} \beta &= (2\rho)^3 \left( \frac{4AD}{\pi kT} \right) \\ &= (2\rho)^3 \left( \frac{4A}{\pi kT} \right) D_0 \exp(-E_m/kT), \end{aligned} \quad (4.25)$$

where,  $E_m$  is the migration energy of the mobile defects. The relations between  $\ln \beta T$  and  $1/T$  should yield straight lines whose slopes give the migration energy.

On the other hand, when point defects are distributed homogeneously, the time  $t$  required for a point defect to drift back from its initial position ( $r, \theta$ ) is

$$\begin{aligned} t &= \frac{kT}{AD} \int_\theta^{\pi/2} r_0^3 \cos^2 \theta d\theta \\ &= \frac{kT}{AD} r_0^3 \left[ \frac{\pi}{4} - \left( \frac{\theta}{2} + \frac{\sin 2\theta}{4} \right) \right]. \end{aligned} \quad (4.26)$$

Instead of equation (4.23), we obtain the amount of pinners which have arrived at time  $t$  per unit length of dislocation,  $N_c(t)$  as

$$\begin{aligned} N_c(t) &= \frac{1}{2} \int_0^{2\pi} \rho_0 r_0^2(\theta) d\theta \\ &= \frac{1}{2} \int_0^{2\pi} \rho_0 t^{2/3} \left( \frac{AD}{kT} \right)^{2/3} \left[ \frac{4}{\pi - (2\theta + \sin \theta)} \right]^{2/3} \\ &= \rho_0 S \left( \frac{AD}{kT} \right)^{2/3} t^{2/3}, \end{aligned} \quad (4.27)$$

where  $\rho_0$  is the volume density of point defects, and  $S$  is the integration value. Substituting equation (4.27) into the GHIL theory,<sup>1)</sup> we have

$$A_I = A_0 [1 + (\beta_c t)^{2/3}]^{-4}, \quad (4.28)$$

where the recovery parameter  $\beta_c$  is given by

$$\beta_c = (\rho_0 S)^{3/2} \left( \frac{4AD}{\pi kT} \right). \quad (4.29)$$

Equation (4.28) may be applicable to such measurements as were carried out immediately after the deformation, because point defects distribute uniformly around the fresh dislocations, and this shows Cottrell Bilby's  $t^{2/3}$  aging law.

### 4.3 Diffusion

It has been considered that the interaction potential of point defects with dislocations is the elastic in the previous section. On the other hand, a divalent impurity in ionic crystals has electric charge. Let us consider a distribution of point defects in the electrical potential of an edge dislocation. The existence probability of vacancy at positive side of divalent impurity  $P_+$ , and at negative side  $P_-$  are

$$P_+ = C_E \exp(E_b + \Delta E)/kT, \quad (4.30)$$

$$P_- = C_E \exp(E_b - \Delta E)/kT, \quad (4.31)$$

where,  $\Delta E$  is given by

$$E = \int_0^a q E dx. \quad (4.32)$$

where  $a$  is the lattice parameter. The dislocation charge is usually negative, and the vacancy is negative at the low temperature. The vacancy-impurity exchange rate  $\nu_+$  and  $\nu_-$  at positive and negative sides of the divalent impurity are

$$\nu_+ = \nu_0 \exp - \frac{E_a + \Delta E}{kT}, \quad (4.33)$$

$$\nu_- = \nu_0 \exp - \frac{E_a - \Delta E}{kT}, \quad (4.34)$$

where  $E_a$  is the exchange energy between the divalent impurity and neighbouring vacancy. If the mean jump frequency of the divalent impurity is designated by  $J_+$  and  $J_-$  for  $P_+$  and  $P_-$ , respectively,

$$J_+ = \nu_+ P_+ = \nu_0 \exp \left( - \frac{E_a + \Delta E}{kT} \right) C_E \exp \frac{E_b + \Delta E}{kT}, \quad (4.35)$$

$$J_- = \nu_- P_- = \nu_0 \exp \left( - \frac{E_a - \Delta E}{kT} \right) C_E \exp \frac{E_b - \Delta E}{kT}. \quad (4.36)$$

Then, both net jump rate becomes

$$J = \nu_0 C_E \exp - (E_a - E_b)/kT. \quad (4.37)$$

The electrical potential  $\Delta E$  disappears, i.e. the electrical potential of dislocations does not affect the migration of divalent impurities. The migration energy for unpinning and pinning process is

$$E_m = E_a - E_b = 0.25 \pm 0.05 \text{ eV}. \quad (4.38)$$

This gives  $E_a = 0.82 \pm 0.05 \text{ eV}$ . Therefore, the migration energy of vacancy  $E_{mc} = E_{II} = 0.709 \text{ eV}$  is smaller than  $E_a$ , and the migration of divalent impurity will be controlled by  $E_a$ , as it was assumed in equation (4.8).

## § 5. Conclusion

The simple conclusion shows that unpinning of divalent-impurities by vibrating breakaway amplitude follows the  $t^{2/3}$  time law. After the sinusoidal breakaway stress is applied on the deformed and aged crystal, the increase in the number of pinning defects on dislocation is proportional to 1/3 power of time in the initial stage of the aging process. On the other hand, the  $t^{2/3}$  time dependency during aging corresponds to the measurement immediately after the deformation, because point defects distribute uniformly around the fresh dislocations. These pinners are considered to be divalent impurity vacancy complexes. In the low-concentration, and the crystal which is not hot enough to be intrinsic, the divalent impurity ion can only diffuse, when it is associated with a vacancy. In the present work, the migration energy of calcium impurity at 15 ppm mol fraction is obtained as  $0.25 \pm 0.05 \text{ eV}$ . The activation energy for the exchange of the calcium impurity and neighbouring vacancy is obtained as  $E_a = 0.82 \pm 0.05 \text{ eV}$ . We conclude that the distribution of divalent-impurity-atmosphere is the distribution of divalent-impurity-atmosphere is only controlled by elastic interaction potential, but not the electrical potential of dislocation.

### Acknowledgements

The author is grateful to Professor S. Yoshida and Professor A. Fukai for helpful discussion.

### References

- 1) A. Granato and K. Lücke: *J. Appl. Phys.* **27** (1956) 705.
- 2) R.H. Chambers and R. Smoluchowsky: *Phys. Rev* **117** (1960) 725.
- 3) D.C. Phillips and P.L. Pratt: *Phil. Mag.* **22** (1970) 809.
- 4) A.H. Cottrell and B.A. Bilby: *Phys. Soc.* **A62** (1949) 49.
- 5) S.H. Carpenter: *Scripta metall.* **3** (1969) 307.
- 6) G. Guenin, J. Perez and P.F. Gobin: *Cryst. Lattice defects*, **3** (1972) 199.
- 7) S.H. Carpenter: *Acta metallurgica*, **16** (1968) 73.
- 8) J.S. Kim, L.M. Slifkin and A. Fukai: *J. Phys. Solids*, **35** (1974) 741
- 9) J. Marx: *Rev. sci. Instrum.* **22** (1951) 503.
- 10) H. Tatenno and H. Taniguchi: *Jpn. J. Appl. Phys.* **19** (1980) 175
- 11) P.W. dreyfus and A.S. Nowick: *Phys. Rev.* **126** (1962) 1367.
- 12) A.S. Nowick: *Point Defect in Solids*, ed. J.H. Crawford, Jr. and L.M. Slifkin (Plenum Press, New York, 1972) Vol. I, p. 151.
- 13) D.L. Kirk and P.L. Pratt: *Proc. Brit. Ceram. Soc.* **9** (1967) 215.
- 14) A. Granato, A. Hikata and K. Lücke: *Acta Metall.* **6** (1958) 470.